Journal of Pipeline Science and Engineering 4 (2024) 100181

Contents lists available at ScienceDirect

Journal of Pipeline Science and Engineering

journal homepage: www.keaipublishing.com/en/journals/journal-of-pipeline-science-and-engineering/

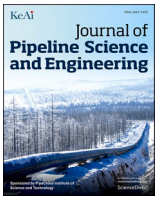

Effect of brine salinity on the partitioning, distribution and corrosion inhibition performance of a quaternary amine corrosion inhibitor

Yasmin Hayatgheib [a], Joshua Owen [a], Raeesa Bhamji [a], Dilshad Shaikhah [a], Jeanine Williams [a], William H. Durnie [b], Mariana C. Folena [c], Abubaker Abdelmagid [c], Hanan Farhat [c], Richard C. Woollam [a], Richard Barker [a,*]

[a] Institute of Functional Surfaces, School of Mechanical Engineering, University of Leeds, Leeds LS2 9JT, UK
[b] bp Australia 240 St. Georges Terrace, Perth, Western Australia
[c] The Corrosion Center of Qatar Environment & Energy Research Institute, Hamad Bin Khalifa University Doha 34110, Qatar

ARTICLE INFO

Keywords:
CO_2 corrosion
Partitioning
Corrosion inhibitors
Water-oil environments
Salinity
Micellisation

ABSTRACT

Surfactant corrosion inhibition performance in water–oil environments is influenced by complex relationships between their physical properties, solution chemistry and interfacial characteristics. The existence of polar heads/nonpolar tails influences both the preferential distribution of the surfactant between the two media as well as the phase in which micellisation occurs. Both phenomena affect the efficiency of the surfactant inhibitor and its adsorption at the metal-solution interface. To demonstrate the complexity of such interactions, the effect of brine salinity on the critical micelle concentration (CMC) and partitioning/distribution behaviour of a quaternary amine corrosion inhibitor (alkyldimethylbenzylhexadecylammonium chloride, or BAC-C_{16}) in a brine and toluene system (at 1:1 ratio) was explored. All experiments were conducted at 50 °C and pH4 over varying salinities (0.1, 1 and 10 wt%) of NaCl brine. Both CMC and partitioning characteristics of BAC-C_{16} are significantly affected by aqueous phase salinity, with an inversion of the partitioning response observed between concentrations of 0.1 and 1 wt% NaCl. The effect of BAC-C_{16} partitioning/distribution behaviour on corrosion inhibitor performance was examined using rotating cylinder electrode experiments. The results illustrate that in order to establish the true corrosion inhibition behaviour, consideration of the chemical distribution characteristics is crucial.

1. Introduction

Corrosion inhibitors provide a cost-effective method for internal corrosion control of carbon and low alloy steel infrastructure within the oil and gas industry (Finšgar and Jackson, 2014). The correct selection and validation of inhibitors are essential to ensure successful, safe and reliable operation of infrastructure. Corrosion inhibitors used in upstream oil and gas production are characteristic of surfactant molecules, which adsorb at the metal-solution interface, creating a dynamic physical barrier that reduces electrochemical dissolution (Sastri, 1998). Many oilfield surfactants are amphiphilic in nature, comprising a charged polar "head" joined to an alkyl chain (typically C_{12}–C_{18}). Such structure is useful in achieving adsorption and effective protection at the metal surface, but also influences surfactant affinity for water-oil-solid interfaces (Sastri, 1998; Rafiquee et al., 2009). The fundamental processes governing surfactant adsorption are key to understanding how corrosion inhibitors function, as the interfacial adsorption properties of such chemistries play a critical role in corrosion protection (Zhu et al., 2017). The adsorption of organic surfactants at a metal-solution interface occurs through the displacement of adsorbed water at the inner Helmholtz plane of the surface, resulting in corrosion inhibition (Sastri, 1998). However, the surfactant properties of many corrosion inhibitors are such that they can influence, as well as be influenced by the physical chemistry of the system, creating added complexity. Two physical properties of surfactant-type corrosion inhibitors that are particularly important to consider in oil and gas production systems are 1) micelle formation, and 2) the partitioning behaviour between oil and water (Woollam et al., 2013).

* Corresponding author.
E-mail address: r.j.barker@leeds.ac.uk (R. Barker).

https://doi.org/10.1016/j.jpse.2024.100181
Received 2 December 2023; Received in revised form 3 February 2024; Accepted 15 February 2024
Available online 20 February 2024

1.1. Micelle formation and the critical micelle concentration (CMC)

As the concentration of monomeric amphiphilic surfactant in solution increases in a given phase, so does the tendency for aggregation. The CMC is defined as the concentration at which micelles begin to form within the bulk solution in a particular phase. Importantly, an increase in total surfactant concentration beyond the CMC promotes little or no change in the concentration of monomer surfactant molecules (Wandelt, 2012). Any further surfactant addition to the system typically contributes to the formation of new or existing micelles (Zhu and Free, 2016; Free, 2002). Thus, little further inhibition efficiency is typically attained through surfactant addition post-CMC compared to pre-CMC. Therefore, the CMC often marks an effective boundary condition in relation to the performance of surfactant-based corrosion inhibitors (Free, 2002; Achour and Kolts, 2015).

1.2. Partitioning behaviour of surfactants

With regards to amphiphilic corrosion inhibitors, the hydrophilic functional group of the surfactant has a strong affinity for the aqueous phase, as well as the steel surface. In contrast, whilst the hydrophobic chain helps establish an effective adsorbed corrosion barrier, its non-polar characteristics promote preferential interaction with hydrophobic entities such as the hydrocarbon phase (Zhu et al., 2015). Such interactions can result in surfactants preferentially dissolving in the hydrocarbon phase and aggregating hydrocarbon chains together, thus depleting surfactant concentration in the aqueous phase and compromising surfactant adsorption at the steel surface (Zhu and Free, 2015). This behaviour can result in a significant reduction in inhibition efficiency, compromising the effectiveness of a corrosion management strategy using chemical treatment.

Fig. 1 illustrates some of the many equilibria that may be involved when a surfactant is present in an aqueous or oil phase with resultant adsorption at the solid-liquid interface. When an aqueous surfactant-containing solution encounters a hydrocarbon phase (such as an oil-water system in a steel pipeline), the surfactant monomer may partition into the oil phase until equilibrium is established. Determining the degree of surfactant partitioning between oil and water is a critical step in understanding corrosion inhibitor performance. Several authors have demonstrated the application of partitioning to the assessment of inhibitors (Zhu and Free, 2015). However, effective measurement in both oil and water phases can be challenging, particularly for commercial corrosion inhibitors which comprise complex mixtures of multiple surfactants (Zhu et al., 2015).

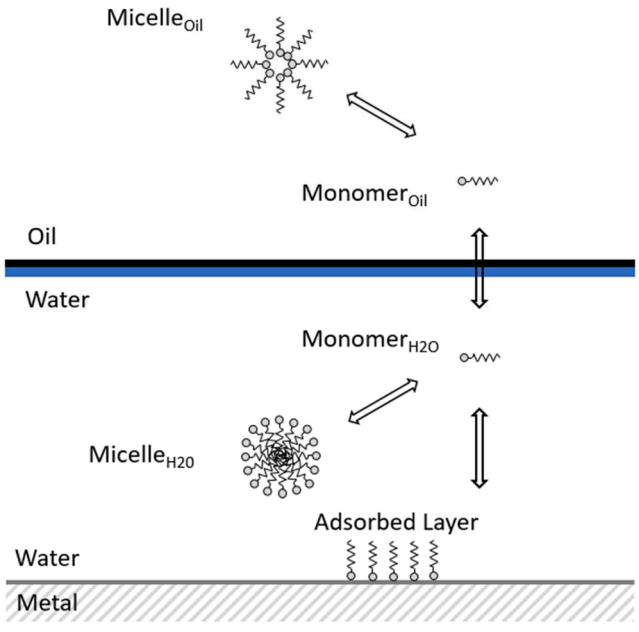

Fig. 1. Schematic of dynamic equilibria established for a surfactant exposed to an oil-aqueous phase system with resultant adsorption to a solid-liquid interface. (Woollam et al., 2013).

For pure surfactants, partitioning is usually characterised by a Partition coefficient (P), shown in Eq. (1), defined as the ratio of monomeric surfactant concentration in oil to that in water ($P_{o/w}$), or vice versa ($P_{w/o}$) (Zhu and Free, 2015):

$$P_{w/o} = \frac{[CI]_{w,m}}{[CI]_{o,m}}, \text{ or } P_{o/w} = \frac{[CI]_{o,m}}{[CI]_{w,m}} \quad (1)$$

Where $[CI]_{o,m}$ is the monomeric surfactant concentration in the hydrocarbon phase, and $[CI]_{w,m}$ is the monomeric surfactant concentration in the aqueous phase. By this definition, a true Partition coefficient is based on relative monomeric concentrations and consequently is not strictly applicable to situations of non-ideal behaviour. This is particularly true in the context of surfactants that aggregate to form micelles (Short et al., 2010).

1.3. Relationship between CMC and partitioning/distribution characteristics

Partitioning behaviour can be complicated by the non-ideality of the surfactant chemistry when the CMC is exceeded; either in the hydrocarbon or the aqueous phase (Leo et al., 1971). Fig. 2 shows an idealised plot of the distribution of a surfactant with a given Partition coefficient. Initially, as the total surfactant concentration in the entire two-phase fluid increases, the concentrations in the aqueous and hydrocarbon phase increase in parallel until micelles form in one of the two phases, i.e., the ratio of monomeric surfactant concentration is constant until the CMC is reached. In Fig. 2, micelles form in the aqueous phase. Beyond this point, further surfactant addition to the system theoretically generates no increase in concentration in the hydrocarbon phase, with any additional surfactant contributing to the formation of micelles in the aqueous phase (Zhu and Free, 2015). The behaviour effectively means that the monomer concentration, and hence the true Partition coefficient (based on monomeric surfactant), does not change. However, the ratio of concentrations in each phase beyond the CMC does give rise to a Distribution coefficient (D_1, D_2 etc.), shown in Eq. (2) which varies with total concentration, unlike the Partition coefficient (Rice et al., 1993):

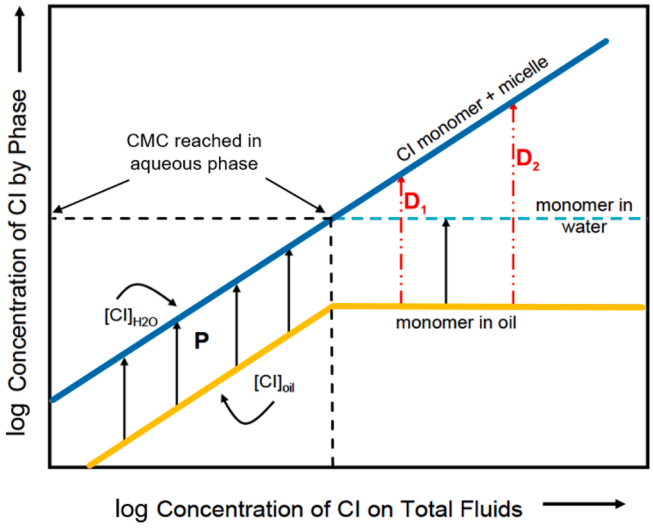

Fig. 2. Graphical illustration of the validity of true Partition coefficient and theoretical surfactant response when micelle formation occurs preferentially in aqueous phase (Woollam et al., 2013).

$$D_{w/o} = \frac{[CI]_{o,t}}{[CI]_{w,t}},\ D_{o/w} = \frac{[CI]_{w,t}}{[CI]_{o,t}} \quad (2)$$

Where $[CI]_{o,t}$ is the total surfactant concentration in the hydrocarbon phase, and $[CI]_{w,t}$ is the surfactant concentration in the aqueous phase (i.e., monomeric and micelle concentration combined).

Extensive research has considered the partitioning characteristics of non-ionic surfactants at low concentrations (i.e., below CMC in either phase) across a variety of conditions (Free, 2002; Achour and Kolts, 2015; Zhu et al., 2015; Zhu and Free, 2015; Short et al., 2010). To properly assess partitioning, the measurement of surfactant concentration in the oil and water phase should be performed in the absence of micelles, i.e., pre-CMC in either phase. This is primarily because analytical techniques are typically unable to differentiate between monomer and micelle-associated surfactant molecules and the partitioning may appear biased if examined post-CMC. Unfortunately, both concepts, i.e., CMC and the inhibitor's preference in partitioning are not always as straightforward as explained above, and factors such as hydrocarbon composition, temperature, salinity, pH, oil type, and presence of other oilfield chemicals and natural surfactants can all have a significant effect on its outcome (Scerbacova et al., 2022; Horsup et al., 2010; Rafique et al., 2020). It is therefore critical to develop a detailed understanding of such factors and their degree of influence on the partitioning behaviour of surfactants (corrosion inhibitors).

1.4. Relevance of brine salinity to surfactant partitioning/distribution

The partitioning characteristic of surfactants at concentrations above CMC has received significant attention predominantly in relation to micro-emulsion formation with relevance to enhanced oil recovery (Aveyard et al., 1986). It is known that the interfacial tension between water and hydrocarbons causes an increase in the capillary force that influences the trapping of hydrocarbon in porous media. Moreover, the interfacial tension between oil and brine is reduced to ultra-low values at an optimum salinity (Clint, 2012). Therefore, through appropriate selection/control of surfactant, co-surfactant and salinity of the aqueous brine, it is possible to generate micro-emulsions at the lowest surface tension, aiding the recovery of residual oil droplets (Aveyard et al., 1986). Fig. 3 schematically illustrates the transition observed when a surfactant-oil-water system composition is kept constant, but the salinity of the aqueous phase varies. At low salinity, two phases form, with the surfactant residing predominantly in the lower phase. At intermediate salinities, there exist three phases, with the majority of the surfactant in the central micro-emulsion phase. At higher salinities, the system reverts to two phases, but with most of the surfactant residing in the oil phase. The lower salinity micro-emulsion is a water-continuous phase containing micelles, whilst the higher salinity micro-emulsion is an oil-continuous phase containing inverted micelles (Davis et al., 1989). Such observations from the enhanced oil recovery literature highlight the key role of salinity in the partitioning characteristics of surfactants (Davis et al., 1989). These inversions in the partitioning response (i.e., preferential micelle formation in the oil phase), especially from corrosion inhibitors' point of view, could become extremely detrimental to infrastructure integrity.

An example of the effect of inversion in the partitioning behavior is shown in Fig. 4, which demonstrates the opposite response to that observed in Fig. 2. In Fig. 4, micelles form in the oil phase. Beyond this point, further surfactant addition to the system generates no increase in concentration in the aqueous phase, with any additional surfactant contributing to the formation of micelles in the oil phase, thus preventing micelle formation within the aqueous phase. The fact that this response prevents the CMC from being reached in the aqueous phase has the potential to severely limit the corrosion inhibitor performance. This is particularly relevant considering the CMC typically marks an effective boundary near which the optimum inhibition performance is attained (Zhu et al., 2017).

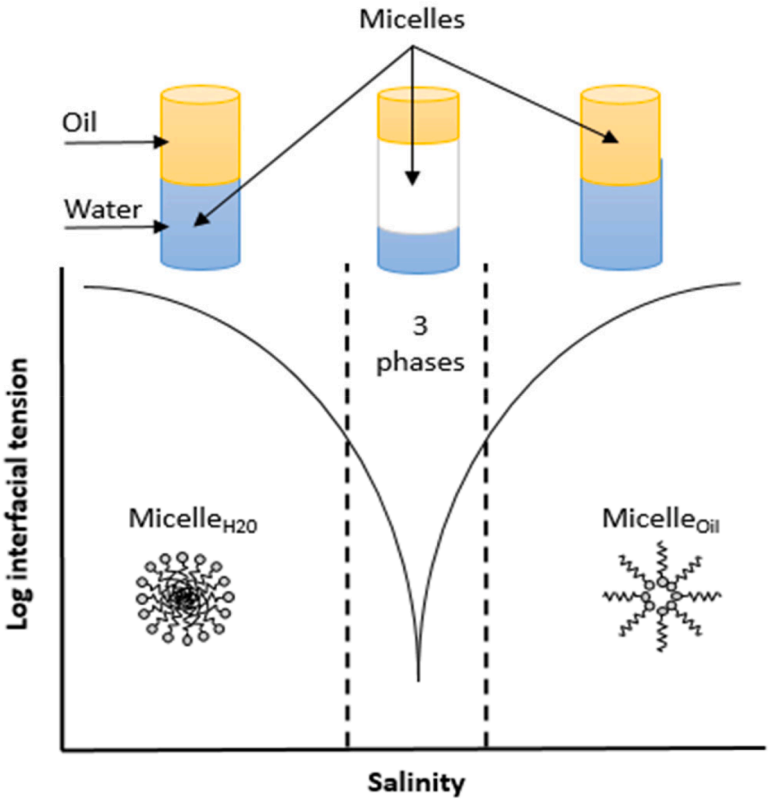

Fig. 3. Sequence of phases produced by inversion from an oil/brine micro-emulsion to a brine/oil micro-emulsion as a result of a change in brine salinity (Clint, 2012).

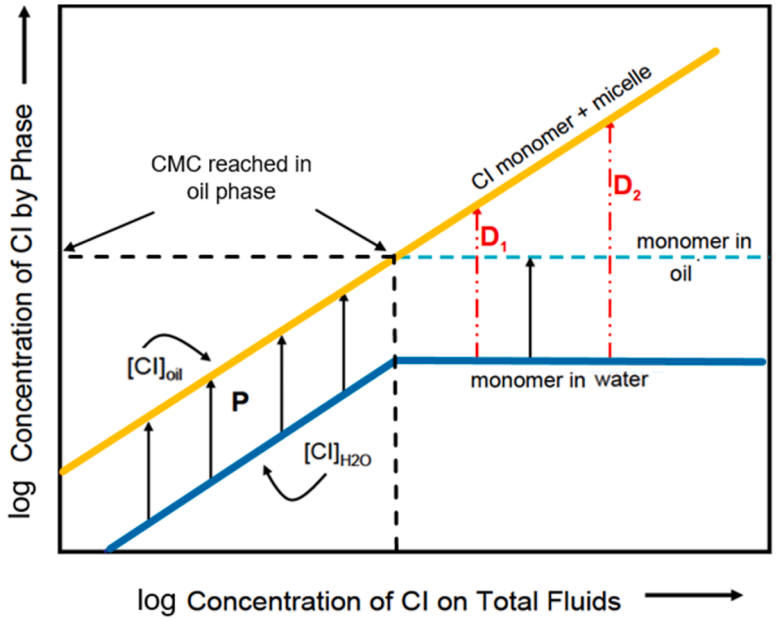

Fig. 4. Graphical illustration of theoretical surfactant response when micellisation occurs preferentially in oil phase (Woollam et al., 2013).

The ability to measure inhibitor concentration in oil and water phases as a means of understanding partitioning behaviour is critical to the successful selection and deployment of corrosion inhibitors in oil and gas systems that require continuous chemical injection. Determining such characteristics directly impacts performance and the determination of appropriate dose rates as a function of water volume fraction. In this work, the effect of brine salinity on the partitioning/distribution behaviour of a quaternary amine corrosion inhibitor molecule (alkyl-dimethylbenzylhexadecylammonium chloride, or BAC-C_{16}) between oil (toluene) and sodium chloride (NaCl) brine and its implications on corrosion inhibition are explored. Firstly, a methodology is introduced and implemented using high-performance liquid chromatography mass spectrometry (HPLC-MS) as a means of direct quantification of surfactant concentration in both the oil and aqueous phase. Subsequently, an existing technique for CMC determination in the aqueous phase using a lipophilic dye is utilised. These two techniques are then used in conjunction with partitioning and rotating cylinder electrode (RCE) experiments to generate a comprehensive understanding of the effect of partitioning/distribution characteristics on inhibitor performance of BAC-C_{16}.

2. Experimental procedure

Development of appropriate methodologies for the determination of both the partitioning characteristics along with the CMC of a corrosion inhibitor provides key information required to assess chemical performance as well as determine distribution in a multiphase system. Such knowledge is critical for the estimation of field-applied dosage rates based on laboratory testing. This paper outlines the procedures and provides results from a series of partitioning experiments to determine the partition characteristics of BAC-C_{16} across a range of brine salinities (0.1, 1 and 10 wt% NaCl brine), which is supported by a series of RCE experiments in the 1 wt% NaCl brine (within the middle of the range) to highlight the implications of such partitioning behaviour on surfactant performance.

2.1. Materials

As stated, the surfactant chosen in this study is BAC-C_{16}, with the structure shown in Fig. 5. BAC-C_{16} with CAS 122-18-9 was purchased from Sigma Aldrich at >99% purity. High-purity toluene (HPLC-grade) with CAS 108-88-3 purchased from Merck was used as the hydrocarbon phase in all partitioning tests. Methanol, Nile red dye (CAS 7385-97-3), formic acid, Hydrochloric acid (HCl) and NaCl salt were also purchased at HPLC-grade, all from Sigma Aldrich.

X65 (UNS K03014) carbon steel coupons were used as the working electrodes (WE) for RCE electrochemical experiments. The chemical composition of the X65 carbon steel used is provided in Table 1, with the microstructure consisting of ferrite and pearlite phases. Prior to the start of each experiment, the surface of the electrode was wet-ground with silicon carbide paper up to 600-grit, degreased with acetone, rinsed with distilled water and dried with compressed air before being placed in the test solution.

2.2. Method development for partitioning experiments

All partitioning tests were performed at 50 °C, with the aqueous phase consisting of pH4, NaCl solution at concentrations of 0.1, 1 and 10 wt%. The testing temperature of 50 °C was chosen such that it was high enough to ensure dissolution of BAC-C_{16} in the aqueous phase, but low enough to enable the surfactant to work effectively as an inhibitor (as performance is known to deteriorate rapidly at higher temperatures). Tests were conducted with a 50:50 vol fraction of the aqueous to hydrocarbon (toluene) phase. Prior to each test, the brine was prepared to the specified concentration (0.1, 1 or 10 wt% NaCl) by mixing analytical grade NaCl with deionized water until dissolved. The brine pH was subsequently adjusted to pH4 using dilute hydrochloric acid. Both the hydrocarbon and brine phases were pre-saturated by adding a sufficient quantity of each to the other to maintain a two-phase system and leaving overnight at room temperature to ensure equilibrium. Pre-saturated fluids were used for all partitioning tests. Stock solutions of BAC-C_{16} with known, precise concentrations (1,000, 10,000 and 100,000 mg/L) were prepared in methanol and were used to achieve the desired concentration of inhibitor in each vial whilst maintaining accuracy. Equal

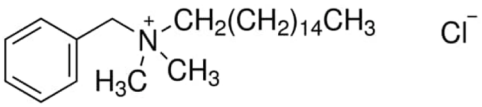

Fig. 5. Structure of BAC-C_{16}, CAS 122-18-9, molecular mass of 395.33 g/mol.

Table 1
Elemental composition of X65 carbon steel (wt%).

C	Mn	Ni	Nb	Mo	Si	V	P	S	Fe
0.15	1.422	0.09	0.054	0.17	0.22	0.06	0.025	0.002	Bal.

known volumes (15 mL) of the pre-saturated aqueous and toluene phases were added to a 40 ml glass vial. A known volume of stock solution, calculated to achieve the desired inhibitor concentration, was added to the vial. Concentration was calculated and specified based on the total volume of both fluids. The concentrations assessed based on the total fluid volume ranged from 2.5 to 500 mg/L (ppm). Each vial was sealed, agitated gently and placed in a water bath at 50 °C for a minimum of 24 h. If no emulsion was detected at the interface, the toluene and brine phases were extracted using a syringe whilst still at the test temperature, i.e., whilst in the water bath at the bath temperature.

2.2.1. Preparation of standards

Standards of BAC-C_{16} (0.1–10 mg/L) were prepared in brine as well as toluene for calibration purposes and were processed with the same exact method explained in Section 2.2. Calibration curves were built for each phase by calculating the peak area under ion abundance (intensity) and chromatogram which was then plotted versus concentration. Example calibration curves, which were constructed prior to every analysis for both phases, are shown in Fig. 6.

2.2.2. Solid phase extraction (SPE) of brine fractions

The brine standards and fractions obtained from each of the partitioning experiments were processed by SPE. Waters Oasis HLB 6 cc (150 mg) extraction cartridges were used to extract the model compounds from the brine samples into methanol with 0.1% (v/v) formic acid for analysis on liquid chromatography with mass spectrometry (LC-MS). The cartridges were placed on an SPE vacuum manifold, solvated with 3 mL methanol and then flushed with 3 mL of deionized water. The sample (5 mL) was loaded onto the cartridge, and eluted with 3 mL of deionized water. The cartridge was allowed to run dry under a vacuum. The model compounds were then eluted from the cartridge using 5 mL of methanol with 0.1% (v/v) formic acid into a 5 mL volumetric flask.

2.2.3. Preparation of toluene fraction for analysis

The toluene standards and fractions were diluted 1:3 with 0.1% (v/v) formic acid in methanol before being analysed by LC-MS.

2.2.4. HPLC methodology for partitioning analyses

LC-MS was used to determine the concentrations of the compounds in the two phases of the partitioning experiments. An Agilent 1290 Infinity II HPLC system was connected to an Agilent 6120B single quadrupole mass spectrometer with an Electrospray Ionization source. The column (Avantor ACE 3 C18, 3 μm, 100 × 3 mm) was kept at 40 °C, and a flow rate of 0.5 mL/min, with 0.1% formic acid and 5 mM ammonium formate in water as solvent A, and 0.1% formic acid in methanol as solvent B. The gradient program started with 50% of solvent A for 0.5 min and then ramped up to 100% of solvent B over 10 min. The 100% of solvent B was maintained for another 5 min and returned to the initial condition (50% solvent A) over 2 min. The prepared samples were injected at a volume of 1 μL. The electrospray ionisation source was run in the positive mode, with the product ion of 360.7 m/z used for selected ion monitoring (SIM) of the BAC-C_{16}.

2.3. Method development for CMC determination

2.3.1. Solution preparation

The CMC was measured using a spectrophotometric method involving the lipophilic dye Nile Red (Kurniasih et al., 2015); this method was selected as the dye probes the micelles directly rather than relying on surface tension as a proxy for micelle detection. The test

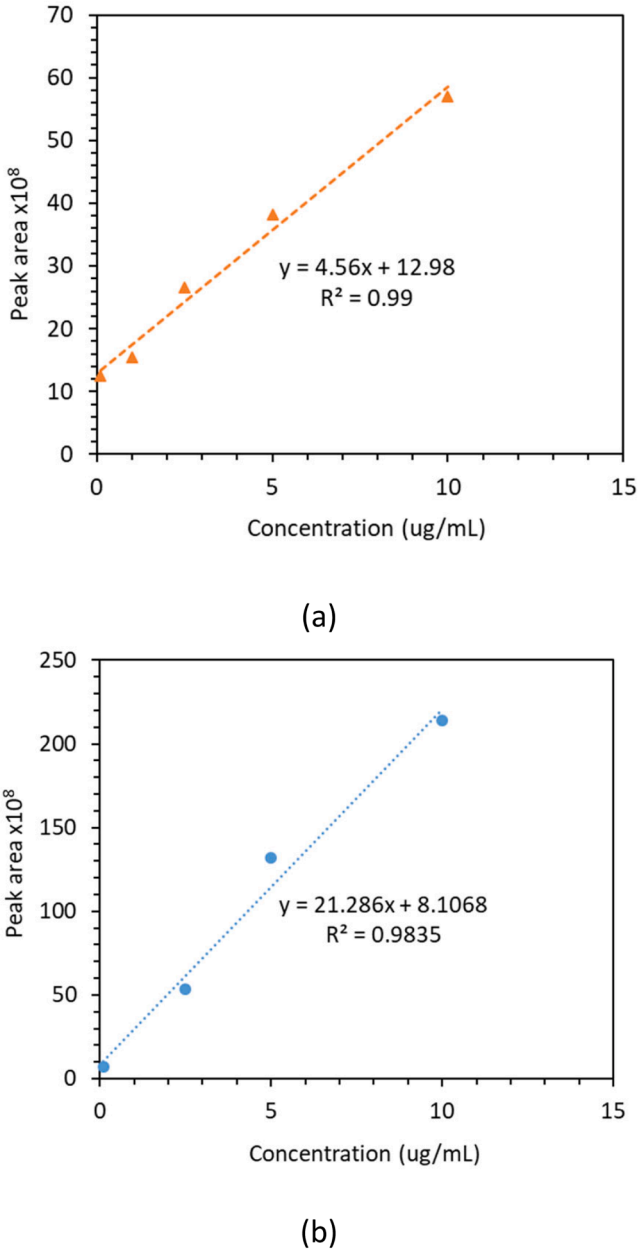

Fig. 6. Example HPLC-MS calibration curve for BAC-C_{16} in (a) toluene and (b) brine phases.

solution was prepared from a concentrated inhibitor stock solution with typically ten times greater concentration than the highest sample concentration evaluated in each mixture experiment. Given the reversible nature of micelle formation, this is a valid approach, providing that the various test solutions formulated at lower concentrations were afforded enough time to re-equilibrate.

To achieve the desired concentration, each sample was prepared by weighing out a minimum required mass of BAC-C_{16} in a 250 mL beaker, dissolving in the appropriate volume of either 0.1, 1 or 10 wt% NaCl brine solution at pH4 (set using 1 M hydrochloric acid). The inhibitor

was dissolved in the solution at 50 °C using a magnetic stirrer to ensure full dissolution. The concentrated stock solution was then combined with either a 0.1, 1 or 10 wt% NaCl solution at pH4 and 50 °C in different ratios and mixed thoroughly for 15 min to achieve approximately 14–20 samples with concentrations spanning two to three orders of magnitude. A 7 mL sample was taken from each of the brine solutions and placed into a sealed vial. A sample with no surfactant was collected in order to initially "zero" the spectrophotometer during measurements. All sealed vials were then stored in a water bath at 50 °C for about 1 h.

2.3.2. Nile Red addition and incubation

Nile Red dye was used to identify the absence or presence of micelles in each collected sample (Kurniasih et al., 2015). Nile Red powder was dissolved in methanol to produce a 1,000 μM concentration dye. 70 μL of dye was pipetted into each 7 mL vial (with the exception of the "zero" sample). After the addition of the dye, each vial was then shaken vigorously for >1 min and placed back in the water bath. After Nile Red had been added to the final sample, the vials were left to incubate in the water bath for 30 min before beginning measurements in the spectrophotometer. One minute was left between Nile Red addition into each sample to account for the time between spectrophotometer readings, to ensure consistent incubation times for every sample.

2.3.3. Spectrophotometer readings

A DR3900 Laboratory Spectrophotometer was used to determine the absorbance spectra across the various concentrations of BAC-C_{16} tested in 0.1, 1 and 10 wt% NaCl brines. After 30 min of incubation, the spectrophotometer readings began with the "zero" samples (containing no inhibitor) to calibrate/zero the spectrophotometer. The readings for all the inhibitor samples were then carried out in order of increasing concentration. Samples were poured into a cuvette and placed in the spectrophotometer which measured the absorbance of each sample across the visible light spectrum from 350 to 800 nm wavelength. A higher concentration of micelles in a sample would result in a greater number of Nile Red molecules either partitioned into the micelles or attached to the micelle structure itself. Owing to the poor solubility of Nile Red in water, the intensity of absorbance in the range 560–590 nm is low and relatively constant in the absence of micelles. However, beyond CMC, the intensity of colour increases proportionally with the log of concentration, resulting in a continuous increase in peak absorbance measurement with a concentration beyond CMC (Kurniasih et al., 2015).

2.3.4. Data analysis/CMC determination

The absorbance spectra for each sample were transferred from the spectrophotometer to a PC. The maximum peak intensity was then extracted in the range 560–590 nm. The associated maximum peak intensity for each spectrum was then plotted against its respective concentration using a logarithmic scale. Two distinct trends were apparent in the plot. At low, pre-CMC concentrations, absorbance was relatively constant with increasing concentration. Further increase in the concentration above CMC resulted in absorbance increasing proportionally with the log of concentration. Trend lines were fitted to the pre-CMC and post-CMC regions and the point of intersection was deemed to be the CMC. Each CMC analysis was repeated a minimum of 3 times.

2.4. Method development corrosion rate determination

2.4.1. Experimental setup

Experiments were conducted in 1 wt% NaCl 1 L solutions at 50 °C and approximately pH4 across a range of selected BAC-C_{16} concentrations, with the use of a 25 mm length magnetic stirrer in the bottom of the vessel, rotating at 500 rpm to ensure thorough mixing of the surfactant within the test solution. Prior to each experiment, the test solution was saturated with CO_2 gas for a minimum of 12 h at room temperature before heating to the desired test temperature. All tests were carried out at atmospheric pressure. A standard three-electrode cell configuration was used within the RCE in order to conduct CO_2 corrosion experiments with the X65 carbon steel coupon serving as the working electrode, a silver/silver chloride (Ag/AgCl) reference electrode and a platinum counter electrode. A 15-minute pre-corrosion period was used prior to inhibitor addition to the test solution. All inhibitors were injected into the test solution using a pipette, after predissolving in a known quantity in methanol.

2.4.2. Corrosion rate measurement

Electrochemical measurements were performed using an Ivium Compactstat potentiostat. Linear polarisation resistance (LPR) measurements were performed for each inhibitor concentration tested. Measurements were performed every 2–3 min by scanning from −5 mV vs. open circuit potential (OCP) to +5 mV vs. OCP at a scan rate of 0.25 mV/s. The corrosion rate at each instance in time was obtained from the measured polarisation resistance using a Stern-Geary coefficient of 26 mV.

3. Results and discussion

3.1. Effect of ionic strength on CMC

The CMC of BAC-C_{16} was determined at different brine salinities with results shown in Fig. 7. Each figure represents one set of data, whilst the CMC value provided represents an average of a minimum of three sets of data. Results indicate that there is a clear reduction in CMC with increasing salinity, with values of 50±4, 23±5 and 12±4 μM determined for salinities of 0.1, 1 and 10 wt%, respectively.

3.2. Effect of ionic strength on partitioning

The effect of ionic strength on partitioning between an aqueous phase and toluene was determined for BAC-C_{16}. Brine salinities of 0.1, 1 and 10 wt% NaCl were studied for a fixed temperature of 50 °C at pH4. The concentrations within each phase were determined using the analysis method reported in the experimental section. This enables the data to be plotted in a similar manner to that of Fig. 2, where the concentration added to the system on a total volume basis is plotted on the *x*-axis and the measured concentration in each of the respective phases is plotted on the *y*-axis.

Fig. 8 shows the partitioning data obtained for BAC-C_{16} as a function of ionic strength. Fig. 8(a) shows a progressive and continuous increase in BAC-C_{16} concentration in the aqueous phase (*y*-axis) as a function of concentration based on total fluid (*x*-axis). In addition, there is a clear point at which the concentration measured in the toluene phase reaches a plateau, whilst the concentration measured in the aqueous phase continues to increase as a function of the concentration based on total volume. The point at which the concentration in the toluene phase begins to plateau is related to the CMC in the aqueous phase, corresponding to the commonly known Winsor I type classification of emulsions, which can be thought of as an oil-in-water micro-emulsion (Winsor, 1948). The dashed lines in Fig. 8(a) show the estimate for CMC determined using the partitioning response (about 45 μM), broadly in agreement with the CMC determined using Nile Red method (50±4 μM). By similar analysis, the CMC in the toluene phase can be determined as 100 and 90 μM for the 1 wt% and 10 wt% NaCl systems, respectively, though these are not independently validated within this work.

A reversal of behavior in Fig. 8(b) is observed as the salinity is increased from 0.1 wt% to 1 wt% NaCl. This response sees the aqueous phase reach a plateau, while the concentration in the toluene phase continues to increase as a function of the concentration based on total fluid volume. This is an important observation; regardless of how much BAC-C_{16} is introduced to the total fluid, the concentration in the brine never exceeds approximately10 μM, which is 40% of the CMC under these conditions. Such behaviour is suggestive of the preferential

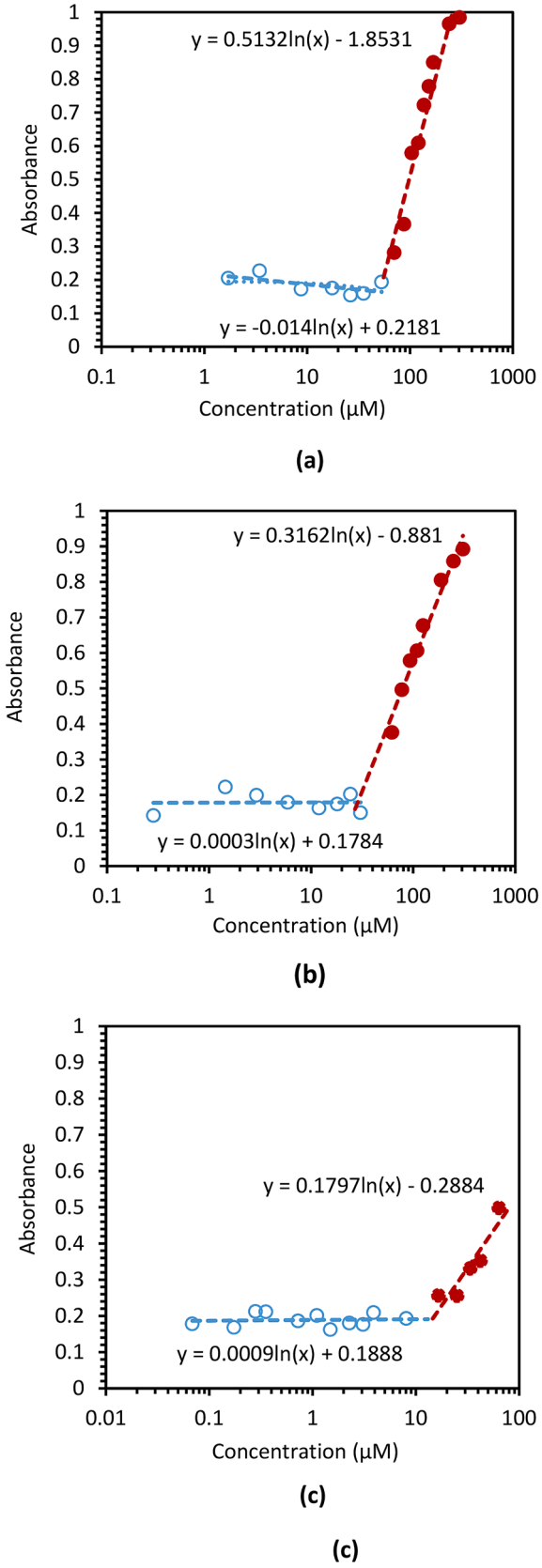

Fig. 7. Peak absorbance in the range 560–590 nm as a function of concentration for BAC-C_{16} at 50 °C, pH4, and brine salinities of (a) 0.1 wt% NaCl, (b) 1 wt% NaCl, and (c) 10 wt% NaCl; pre-CMC in blue, open circles and post-CMC in red, solid circles: transition points were consistently observed at concentrations of (a) 50±4 μM, (b) 23±5 μM and (c) 12±4 μM.

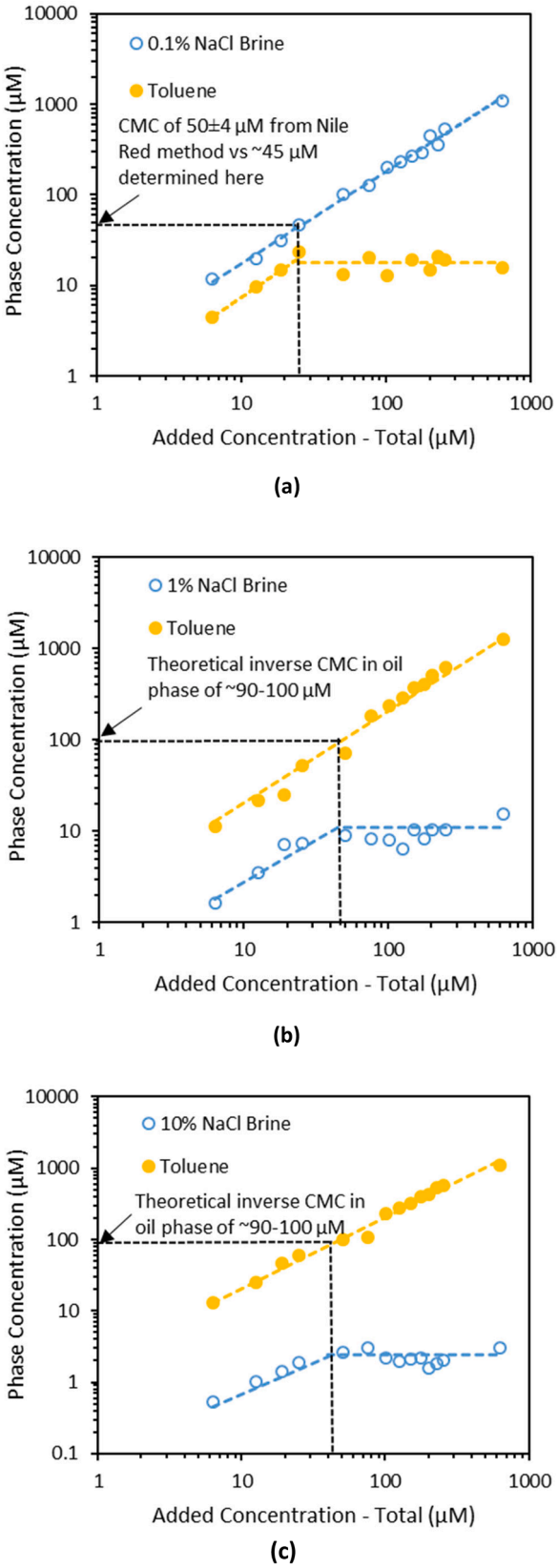

Fig. 8. Partitioning data for BAC-C_{16} between (a) 0.1 wt% NaCl brine and toluene, (b) 1 wt% NaCl brine and toluene and (c) 10 wt% NaCl brine and toluene.

formation of micelles in the toluene phase, i.e., inverse micelle formation in the hydrocarbon phase. This is not unexpected given the increase in salinity, which increases the formation of a Winsor II system occurring, which can be thought of as a water-in-oil micro-emulsion (Winsor, 1948). In Fig. 8(c), the Winsor II system is again observed with a 10 wt% NaCl brine. However, the plateau in BAC-C_{16} concentration results in surfactant concentration being restricted to a maximum of about 2 μM in the brine phase. These observations from Fig. 8 highlight the key role of salinity in the partitioning characteristics of surfactants, with Fig. 8(b) and Fig. 8(c) reiterating the effect of inversion in the partitioning response shown previously in Fig. 4.

Fig. 9 shows the calculated Partition coefficient ($P_{w/o}$) and Distribution coefficient ($D_{w/o}$) from Eqs. (1) and (2) for all three environments of 0.1, 1 and 10 wt% salinity. The *x*-axis represents the total concentration of surfactant added to each test vial containing 1:1 (v/v) brine-toluene. As explained earlier, $P_{w/o}$ represents the surfactant ratio in the form of monomers, which is constant for both phases before the CMC (as illustrated with the use of dashed lines on Fig. 9). However, $D_{w/o}$ represents the total surfactant ratio (in the form of monomers and micelles), which is consistent with $P_{w/o}$ pre-CMC, but deviates from $P_{w/o}$ after micellisation in either of the two phases. Depending on the preferential partitioning of the surfactant (which is influenced by salinity), $D_{w/o}$ can show an increasing or decreasing trend. As shown in Fig. 9, for 0.1 wt% NaCl, where surfactant micelles form in the brine phase, $D_{w/o}$ has an increasing trend beyond CMC. The total concentration at which the calculated $D_{w/o}$ values begin to increase (i.e., around 20–25 μM) relates to the CMC in the brine phase (about 45 μM – as shown in Fig. 8) which is independently validated by CMC measurements using the Nile red test (50±4 μM). As for the higher salinity environments, i.e., 1 wt% and 10 wt%, $D_{w/o}$ shows an decreasing trend beyond a given concentration. In these cases, as explained in Fig. 8, the point of deviation of $D_{w/o}$ from $P_{w/o}$ represents the CMC in the toluene phase. For both 1 and 10 wt% NaCl where micellisation occurs in the toluene phase, the points of deviation for both systems are very close to one another, i.e., in the total concentration range of 45–50 μM, corresponding to between 90 and 100 μM in the toluene phase for the 1 wt% and 10 wt% NaCl systems. Furthermore, it is worth noting that the Partition coefficient ($P_{w/o}$) determined in Fig. 9 for each system decrease with the increasing salinity of the system. Such behaviour is expected, as at low salinity the partitioning of BAC-C_{16} is more inclined to the brine phase.

3.3. Relating partitioning characteristics to corrosion inhibitor performance

A series of RCE corrosion experiments were performed in exclusively the aqueous phase of the 1 wt% NaCl system with no toluene present in order to determine the influence the partitioning characteristics have on inhibitor performance. The concentrations selected for the corrosion experiments corresponded to :

1) the maximum concentration which BAC-C_{16} is limited to in the 1 wt% NaCl brine phase as a result of its partitioning characteristics, as shown in Fig. 8(b), which is 10 μM;
2) the CMC of BAC-C_{16} in 1 wt% NaCl phase, which is 23 μM;
3) a nominal value which is approximately 4 times the CMC, i.e., 100 μM.

The inhibition performance for BAC-C_{16} at concentrations of 10, 23 and 100 μM as a function of time is provided in Fig. 10, with the inhibitor being introduced after 15 min of pre-corrosion. Referring back to Fig. 8(b), the maximum concentration of BAC-C_{16} reached in the aqueous phase is about 10 μM. The typical performance of the surfactant at this concentration is shown in Fig. 10, where a period of initial adsorption is observed, followed by progressive desorption, resulting in an end-point inhibition efficiency typically of <10%. Such observations were consistent from multiple repeat experiments, with some experiments showing no inhibitive effect from BAC-C_{16}. Increasing the concentration to 23 μM produced an efficiency of about 80% (0.60 mm/a), whilst tests at 100 μM showed that a further increase in surfactant inhibition performance is possible beyond CMC, reaching around 96% efficiency and a corrosion rate of 0.15 mm/a at the end of the experiment.

It is important to note that while a higher concentration beyond the CMC of BAC-C_{16} leads to greater inhibition efficiency, the incremental improvement in performance from CMC (23 μM) to 100 μM is considerably smaller (about 0.4 mm/a reduction) compared to the enhancement observed when going from 0 to CMC (23 μM) (about 2.7 mm/a reduction). Additionally, achieving this higher efficiency beyond CMC comes with the trade-off of introducing a significantly larger quantity of surfactant into the system.

Assuming the presence of the inhibitor in the aqueous is predominantly responsible for driving/ensuring corrosion protection, Fig. 10

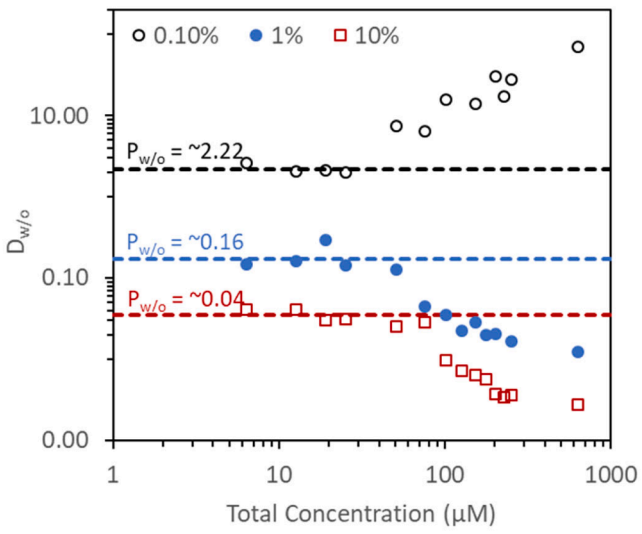

Fig. 9. Plotted partitioning and Distribution coefficient for 0.1, 1 and 10 wt% salinity brine-toluene system at various BAC-C_{16} concentrations.

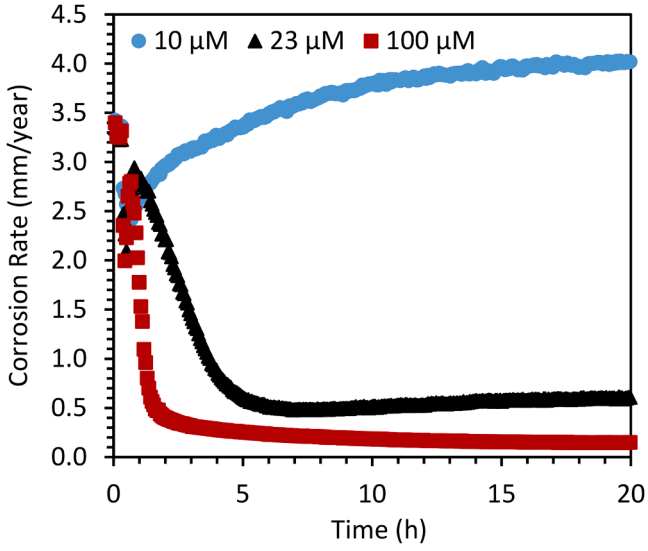

Fig. 10. Corrosion rate vs. time for X65 carbon steel exposed to a CO_2-saturated 1 wt% NaCl brine solution in the presence of varying concentrations of BAC-C_{16}; inhibitor addition was performed after 15 min of pre-corrosion.

suggests that the partitioning behavior of BAC-C_{16} (which limits its concentration in the 1 wt% brine phase to 10 μM) would severely limit its performance. In addition, Fig. 10 shows that a reduction in brine surfactant concentration as a result of partitioning not only restricts BAC-C_{16}'s maximum achievable steady-state coverage/efficiency, but also reduces the rate of adsorption i.e., the experiment at 23 μM takes about 3–4 times longer to reach 50% of the steady-state coverage compared to the experiment at 100 μM.

3.4. Correlating partitioning data with surface coverage

To provide a more comprehensive approach towards relating corrosion inhibition performance to partitioning, further experiments both above and below the concentrations shown in Fig. 10 were performed (i.e., 2, 5, 200 and 500 μM). From each experiment, the minimum corrosion rate obtained during the course of each 20 h experiment was extracted from the corrosion response and used in Eq. (3) to determine the level of surface coverage, θ, achieved at each concentration.

$$\theta = \left(1 - \frac{V_{in}}{V_{un}}\right) \tag{3}$$

Where V_{in} is the corrosion rate observed at the end of the experiment, and V_{un} is the average corrosion rate obtained during the 15 min pre-corrosion.

Whilst no electrochemical experiments on the steel coupons were conducted in a combined two-phase (i.e., toluene-brine) environment, it is useful to compare the partitioning response and the associated corrosion inhibition performance. Fig. 11 summarises the corrosion inhibition performance extracted from the RCE experiments for BAC-C_{16}. The data is plotted as surface coverage (determined using Eq. (3)) vs. concentration, and a trend line is established using the Langmuir isotherm model, exhibiting the form shown in Eq. (4):

$$\theta = \frac{\theta_{max} K_{ads}[CI]}{1 + K_{ads}[CI]} \tag{4}$$

Where K_{ads} is the adsorption equilibrium constant (μM^{-1}); [CI] is the concentration of BAC-C_{16} (μM); and θ_{max} is the maximum surface coverage as [inhibitor] → ∞. The use of the Langmuir isotherm fit enables a continuous curve to be used to represent the relationship between the surface coverage of the inhibitor on the coupon and concentration, producing values of θ_{max} = 0.99 and K_{ads} = 0.040, 3 μM^{-1}. Fig. 11 illustrates that BAC-C_{16} can provide very high levels of surface coverage, reaching in excess of 0.96 (96% efficiency) at concentrations above 500 μM in the brine phase.

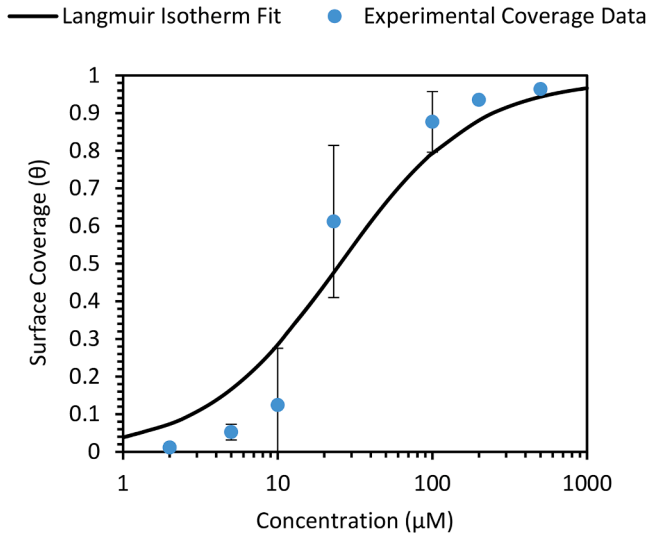

Fig. 11. Corrosion inhibition performance and Langmuir isotherm fit for BAC-C_{16} in 1 wt% NaCl brine at pH4, 50 °C and 1,000 rpm.

Assuming that inhibition from BAC-C_{16} is provided solely by its presence in the aqueous phase, it is possible to estimate its performance in the two-phase system by combining the coverage vs. concentration data in Fig. 11 with that of the partitioning response for the toluene-brine system determined in Fig. 8(b). The combined data and anticipated responses are provided in Fig. 12, which correlates the aqueous partitioning data with that of the corrosion inhibition performance curves. In Fig. 12, the *x*-axis now corresponds to the total concentration of BAC-C_{16} based on the bulk fluid. The upper graph represents the aqueous partitioning response from the model (solid black line) and the experimental HPLC-MS data is provided by the markers. The dashed line in the upper graphs of Fig. 12 indicates the partitioning response that would be observed in the absence of micelle formation in the oil phase. The lower graph within Fig. 12 represents the inhibitor coverage response based on data from Fig. 11, plotted as a function of total surfactant loading, and hence adjusted accordingly by accounting for the quantity of inhibitor partitioning into the aqueous phase. Again, the solid black line in the lower graph represents the response observed practically based on the known distribution characteristics of each surfactant, whilst the dashed line indicates the unrestricted performance of the corrosion inhibitor if micelles never form in the toluene phase, i.e., the response observed if surfactant concentration in the aqueous phase remains unrestricted.

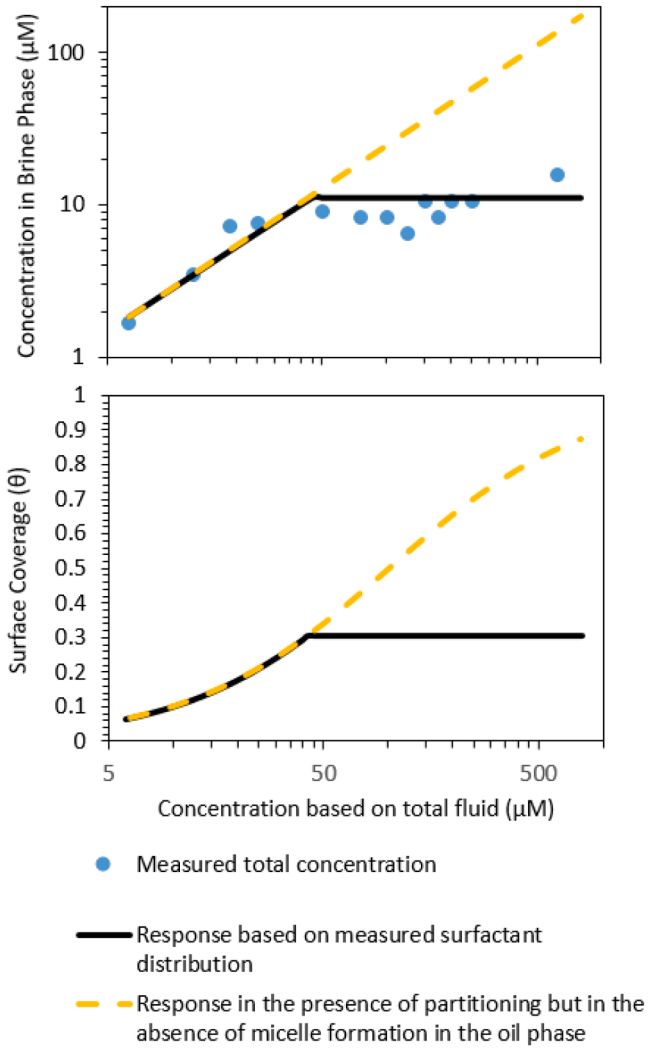

Fig. 12. Comparison of partitioning behaviour and corrosion inhibition tests for BAC-C_{16} in 1 wt% NaCl brine at pH4, 50 °C and 1,000 rpm.

In Fig. 12, the lower graph indicates that the performance of BAC-C_{16} in the presence of partitioning, but in the absence of micellization is extremely good; at a total fluid concentration of 800 μM an efficiency of 90% is attained. However, this level of performance is only reached in the absence of micellization in the toluene phase. In reality, beyond a total fluid concentration of about 45 μM, micelles form in the toluene phase, restricting the concentration of BAC-C_{16} in the aqueous phase is to about 10 μM (upper graphs of Fig. 7(b)). The preferential partitioning into the toluene phase thereby limits the efficiency of BAC-C_{16} to about 30%, preventing the chemical from reaching its maximum inhibition performance.

4. Conclusions

This paper demonstrates the complexity of the interactions and inter-relationship between surfactant CMC, partitioning/distribution, and inhibitor performance for a quaternary amine corrosion inhibitor molecule (alkyldimethylbenzylhexadecylammonium chloride, or BAC-C_{16}). The effect of solution salinity on BAC-C_{16} partitioning/distribution behaviour at 50 °C and pH4 is explored for a brine/toluene system, with the implications of such behaviour determined in the context of interfacial adsorption and inhibition performance. From the study, the following conclusions can be made:

1) A lipophilic dye was used to determine the CMC of BAC-C_{16} as a function of brine salinity. An increase in brine salinity resulted in a distinct reduction in the CMC of BAC-C_{16}.
2) An analytical methodology using HPLC-MS was implemented to quantify BAC-C_{16} concentration in NaCl aqueous systems as well as in toluene.
3) An examination of the partitioning response of BAC-C_{16} between 0.1, 1 and 10 wt% NaCl and toluene using the analytical method supported the theory relating to a 'break point' being observed, i.e., the point where the concentration in one of the two phases plateaus despite the total fluid concentration increasing.
4) In the 0.1 wt% NaCl brine-toluene system, micellisation was observed in the aqueous phase, resulting in a plateau in concentration in the toluene phase. The "break point" was shown to correlate with aqueous CMC determined using the Nile Red method, and hence is suggested to be attributable and indicative of aggregation.
5) A reversal in partitioning behaviour was observed in the 1 and 10 wt% NaCl brine systems with toluene, with the formation of inverse micelles in the toluene phase. This response limited the concentration in the aqueous phase of the 1 and 10 wt% systems to about 10 and 2 μM, respectively, regardless of the quantity of BAC-C_{16} introduced to the total fluid. Both these plateau values are well below the determined aqueous CMC values of 23±5 μM and 12±4 μM, respectively.
6) Corrosion experiments in CO_2-saturated, 1 wt% NaCl brine using an rotating cylinder electrode were performed to understand the impact of distribution on corrosion inhibitor performance. Despite BAC-C_{16} being capable of attaining inhibitor efficiencies in excess of 95% at aqueous concentrations of about 500 μM, its concentration in the 1 wt% NaCl phase was limited to 10 μM in as a result of micellisation in the toluene phase. As a result, the distribution response severely limited the maximum corrosion inhibition potential of BAC-C_{16}, restricting inhibition efficiency to <30%.
7) The work demonstrates that in systems containing both oil and water phases, to determine the true corrosion inhibition performance, the chemical distribution and micellisation characteristics should be understood. Marginal changes in the physical chemistry (salinity in this instance) can have significant consequences in terms of corrosion inhibitor performance, and consequently, asset integrity. These effects not only influence the chemical performance in terms of efficiency, but can also slow the adsorption kinetics through reduction in the aqueous phase concentration.

Data availability

The raw/processed data required to reproduce these findings cannot be shared at this time as the data also forms part of an ongoing study.

CRediT authorship contribution statement

Yasmin Hayatgheib: Writing – review & editing, Writing – original draft, Methodology, Data curation. **Joshua Owen:** Writing – review & editing, Investigation. **Raeesa Bhamji:** Methodology, Formal analysis, Data curation. **Dilshad Shaikhah:** Methodology, Formal analysis, Data curation. **Jeanine Williams:** Writing – review & editing, Methodology, Formal analysis, Data curation. **William H. Durnie:** Writing – review & editing, Supervision. **Mariana C. Folena:** Writing – review & editing, Supervision. **Abubaker Abdelmagid:** Writing – review & editing, Supervision. **Hanan Farhat:** Writing – review & editing, Supervision, Funding acquisition. **Richard C. Woollam:** Writing – review & editing, Writing – original draft, Supervision, Methodology, Investigation, Funding acquisition, Formal analysis, Data curation, Conceptualization. **Richard Barker:** Writing – review & editing, Writing – original draft, Supervision, Methodology, Investigation, Funding acquisition, Formal analysis, Data curation, Conceptualization.

Declaration of competing interest

The authors declare that they have no known competing financial interests or personal relationships that could have appeared to influence the work reported in this paper.

Acknowledgements

This research was supported by the Qatar Environmental and Energy Research Institute (QEERI). The authors would like to express their appreciation for the technical expertise provided by colleagues at QEERI Corrosion Center.

References

Achour, M., Kolts, J., Corrosion control by inhibition Part I: corrosion control by film forming inhibitors, Corrosion 2015 (Dallas, TX, 2015, Paper Number: NACE-2015-5475).
Aveyard, R., Binks, B.P., Clark, S., Mead, J., 1986. Interfacial tension minima in oil-water-surfactant systems behaviour of alkane-aqueous NaCl systems containing aerosol OT. J. Chem. Soc. Faraday Trans. 1 F 82, 125–142.
Clint, J.H., 2012. Surfactant Aggregation. Springer, Netherlands.
Davis, H.T., Bodet, J.F., Scriven, L.E., Miller, W.G., 1989. Microstructure and transport in midrange microemulsions. Physica A 157 (1), 470–481.
Finšgar, M., Jackson, J., 2014. Application of corrosion inhibitors for steels in acidic media for the oil and gas industry: a review. Corros. Sci. 86, 17–41.
Free, M.L., 2002. Understanding the effect of surfactant aggregation on corrosion inhibition of mild steel in acidic medium. Corros. Sci. 44 (12), 2865–2870.
Horsup, D.I., Clark, J.C., Binks, B.P., Fletcher, P.D.I., Hicks, J.T., 2010. The fate of oilfield corrosion inhibitors in multiphase systems. Corrosion 66 (3), 036001.
Kurniasih, I.N., Liang, H., Mohr, P.C., Khot, G., Rabe, J.P., Mohr, A., 2015. Nile red dye in aqueous surfactant and micellar solution. Langmuir 31, 2639–2648.
Leo, A., Hansch, C., Elkins, D., 1971. Partition coefficients and their uses. Chem. Rev. 71 (6), 525–616.
Rafique, A.S., Khodaparast, S., Poulos, A.S., Sharratt, W.N., Robles, E.S.J., Cabral, J.T., 2020. Micellar structure and transformations in sodium alkylbenzenesulfonate (NaLAS) aqueous solutions: effects of concentration, temperature, and salt. Soft. Matter. 16 (33), 7835–7844.
Rafiquee, M.Z.A., Khan, S., Saxena, N., Quraishi, M.A., 2009. Investigation of some oleochemicals as green inhibitors on mild steel corrosion in sulfuric acid. J. Appl. Electrochem. 39 (8), 1409–1417.
Rice, N.M., Irving, H.M.N.H., Leonard, M.A., 1993. Nomenclature for liquid-liquid distribution (solvent extraction). Pure Appl. Chem. 65 (11), 2373–2396.
Sastri, V.S., 1998. Corrosion Inhibitors: Principles and Applications. Wiley, New York.
Scerbacova, A., Kopanichuk, I., Cheremisin, A., 2022. Effect of temperature and salinity on interfacial behaviour of alkyl ether carboxylate surfactants. Pet. Sci. Technol. 41, 1–20.
Short, J., Roberts, J., Roberts, D.W., Hodges, G., Gutsell, S., Ward, R.S., 2010. Practical methods for the measurement of log*P* for surfactants. Ecotoxicol. Environ. Saf. 73 (6), 1484–1489.
Wandelt, K., 2012. Surface and Interface Science. Wiley-VCH, Weinheim.

Winsor, B.P.A, 1948. Hydrotropy, solubilisation and related emulsification processes. Trans. Faraday Soc. 44, 376–398.

Woollam, R.C., Durnie, W.H., Gough, M.A, 2013. Physical chemistry versus oilfield lore: the key to demystifying corrosion inhibition. Corrosion 2013 (Orlando, FL, 2013, Paper Number: NACE-2013-2802).

Zhu, Y., Free, M.L., 2015. Experimental investigation and modeling of the performance of pure and mixed surfactant inhibitors: partitioning and distribution in water-oil environments. J. Electrochem. Soc. 162 (14), 702–717.

Zhu, Y., Free, M.L., 2016. Experimental investigation and modeling of the performance of pure and mixed surfactant inhibitors: micellization and corrosion inhibition. Colloids Surf. A: Physicochem. Eng. Aspects 489, 407–422.

Zhu, Y., Free, M.L., Woollam, R.C., Durnie, W.H., 2017. A review of surfactants as corrosion inhibitors and associated modelling. Prog. Mater. Sci. 90, 159–223.

Zhu, Y., Free, M.L., Yi, G., 2015. Experimental investigation and modeling of the performance of pure and mixed surfactant inhibitors: aggregation, adsorption, and corrosion inhibition on steel pipe in aqueous phase. J. Electrochem. Soc. 162 (10), 582–591.